Electronic Supplementary Material (ESI) for Chemical Communications.

Supporting Information

Copper(II) tetrakis(pentafluorophenyl) porphyrin: Highly Active Copper-based Molecular Catalyst for Electrochemical CO_2 Reduction

Kento Kosugi,[a] Hina Kashima, [a] Mio Kondo,[abc*] Shigeyuki Masaoka[ab*]

[a] Division of Applied Chemistry, Graduate School of Engineering, Osaka University, 2-1 Yamadaoka, Suita, Osaka 565-0871, Japan

[b] Innovative Catalysis Science Division, Institute for Open and Transdisciplinary Research Initiatives (ICS-OTRI), Osaka University, Suita, Osaka 565-0871, Japan

[c] PRESTO, Japan Science and Technology Agency (JST), 4-1-8 Honcho, Kawaguchi, Saitama 332-0012, Japan

Table of contents

1. Experimental details.....S4

General procedures.....S4

Syntheses.....S4

Electrochemistry.....S5

Controlled potential electrolysis (CPE).....S5

X-ray crystallography.....S5

2. Single crystal X-ray structure determination.....S7

Fig. S1.....S7

Table S1.....S8

3. Electrochemical properties.....S9

Fig. S2.....S9

Table S2.....S9

Fig. S3.....S10

4. Quantum chemical calculation.....S11

5. Controlled potential electrolysis experiment.....S12

Fig. S4.....S12

Fig. S5.....S13

Table S3.....S13

6. Evidence for a homogeneous electrocatalyst.....S14

6.1 Dynamic light scattering measurement after the CPE experiment.....S14

Fig. S6.....S14

6.2 UV-visible absorption spectra before and after CPE experiments.....S15

Fig. S7.....S15

6.3 Catalytic ability of the electrode after the CPE experiment.....S16

Fig. S8.....S16

Table S4.....S16

7. TOF calculation S17

7.1 TOF calculation by CPE experiments S17

7.2 Catalytic Tafel plot S18

Table S5 ..... S18

7.3 Comparison of TOF values on CO_2 reduction catalyst S19

Table S6 ..... S19

Fig. S9 ..... S20

8. Catalytic ability of CuTPP S21

8.1 Cyclic voltammetry measurement of CuTPP S21

Fig. S10 ..... S21

8.2 CPE experiment of CuTPP S22

Fig. S11 ..... S21

Table S7 ..... S22

8.3 TOF of CuTPP S22

9. References S23

1. Experimental details

General procedures

Pyrrole was purchased from Sigma-Aldrich Co., LLC. Benzaldehyde and ferrocene were purchased from Wako Pure Chemical Industries, Ltd. Propanoic acid was purchased from Kishida Chemical Co., LLC. Methanol, chloroform ($CHCl_3$), *N*, *N*-dimethylformamide (DMF), hexane, acetonitrile (MeCN) and copper(II) acetate monohydrate ($Cu(OAc)_2 \cdot H_2O$) were purchased from Kanto Chemical Co., Inc. 5,10,15,20-Tetrakis(pentafluorophenyl)porphyrin (**H_2TPFP**), tetra-*n*-butylammonium perchlorate (TBAP), tetra-*n*-butylammonium acetate (TBAA), 2,2,2-trifluoroethanol and were purchased from Tokyo Chemical Industry Co., Ltd. Chloroform-d_1 was purchased from Cambridge Isotopes, Inc. All solvents and reagents are of the highest quality available and used as received except for TBAP. TBAP was recrystallized from absolute ethanol. ^{1}H-NMR spectra were collected at room temperature on a JEOL JNM-ECS400 spectrometer. Elemental analysis was performed on a J-SCIENCE LAB MICRO CORDER JM10 elemental analyzer.

Syntheses

Synthesis of meso-tetraphenylporphyrin (H_2TPP)

H_2TPP was prepared as previously described.[S1] Pyrrole (1.7 mL, 25 mmol) and benzaldehyde (2.6 mL, 25 mmol) were dissolved in propanoic acid (50 mL), then refluxed for 45 minutes and cooled to room temperature. The resulting mixture was filtered and washed with methanol. Recrystallization from $CHCl_3$/methanol gave a purple solid (785 mg, yield 20%). ^{1}H-NMR (400 MHz, $CDCl_3$): d = 8.82 (s, 8H), 8.19-8.21 (m, 8H), 7.71-7.78 (m, 12H), –2.80 (s, 2H) ppm. Elemental analysis Calcd. for $C_{44}H_{30.5}N_4O_{0.25}$ (**H_2TPP**$\cdot$0.25 H_2O): C, 85.34%; H, 4.96%; N, 9.05%. Found: C, 85.24%; H, 4.68%; N, 9.08%.

Synthesis of copper(II) tetraphenylporphyrin (CuTPP)

CuTPP was prepared by the modification of a previous report.[S2] To a solution of **H_2TPP** (50 mg, 0.08 mmol) in DMF (5 mL), a 5 mL DMF solution of $Cu(OAc)_2 \cdot H_2O$ (80.9 mg, 0.41 mmol) was added at room temperature. The mixture was heated at 200 ˚C for 10 minutes by a microwave reactor. Water (50 mL) was added to the resulting solution. Precipitate was collected by filtration and washed with water. Recrystallization from $CHCl_3$/hexane gave a red solid (37.5 mg, yield 68%). Elemental analysis Calcd. for $C_{44}H_{30}CuN_4O$ (**CuTPP**$\cdot$1.0 H_2O): C, 76.12%; H, 4.36%; N, 8.07%. Found: C, 75.98%; H, 4.14%; N, 8.19%.

Synthesis of copper(II) tetrakis(pentafluorophenyl)porphyrin (CuTPFP)

CuTPFP was prepared by the modification of a previous report.[S2] To a solution of **H_2TPFP** (50 mg, 0.08 mmol) in DMF (5 mL), a 5 mL DMF solution of $Cu(OAc)_2 \cdot H_2O$ (30.5 mg, 0.153 mmol) was added at room temperature. The mixture was heated at 200 ˚C for 10 minutes by microwave reactor. Water (50 mL) was added to the resulting solution. Precipitate was collected by filtration and washed with water.

Recrystallization from $CHCl_3$/hexane gave a red solid (37.5 mg, yield 71%). Since this crystal was not suitable for single crystal X-ray structure analysis, **CuTPFP** was also recrystallized from MeCN/H_2O to give a large red plate. Elemental analysis Calcd. for $C_{47}H_{14}F_{20}CuN_4$ (**CuTPFP**·0.5 hexane): C, 52.36%; H, 1.31%; N, 5.20%. Found: C, 52.51%; H, 1.54%; N, 5.51%.

Electrochemistry

Electrochemical experiments were performed at room temperature on a BAS ALS Model 650DKMP electrochemical analyzer or a Bio-Logic-Science Instruments potentiostat. Cyclic voltammetry (CV) measurements were performed by using a one-compartment cell with a three-electrode configuration, which consisted of a glassy carbon disk (diameter 3 mm, BAS Inc.), platinum wire, and Ag/Ag^+ electrode (Ag/0.01 M $AgNO_3$) as the working, auxiliary, and reference electrodes, respectively. The glassy carbon disc working electrode was polished using 0.05 μm alumina paste (BAS Inc.) and washing with purified H_2O prior to each measurement. Ferrocene was used as an internal standard and all potentials are referenced to the ferrocenium/ferrocene (Fc/Fc^+) couple at 0 V.

Controlled potential electrolysis (CPE)

CPE was performed in a gas-tight two-compartment electrochemical cell, where the first compartment held the carbon plate working electrode (1.2 cm^2 surface area) and Ag/Ag^+ reference electrode (Ag/0.01 M $AgNO_3$) in 5 ml of 0.1 M TBAP/solvent (DMF or MeCN) with catalyst and proton source, while the second compartment held the Pt auxiliary electrode in 5 ml of 0.1 M TBAP/solvent (DMF or MeCN) containing TBAA (0.2 M) as sacrificial oxidant. The two compartments were separated by a Nafion® membrane. The solution was purged vigorously with CO_2 for 30 mins prior to electrolysis. The electrolysis experiment was performed for 1 h under constant stirring. The amount of CO and H_2 produced was quantified from an analysis of the headspace with Shimadzu GC-8A with TCD detector equipped with a capillary column with Molecular Sieve 13X-S 60/80. Calibration curves were made by sampling known amounts of H_2 and CO.

X-ray crystallography

Single crystal X-ray diffraction data were collected on a Synergy Custom system CCD Plate equipped with confocal monochromated Mo-Kα radiation (λ = 0.71069 Å) coated with Paratone-N (Hampton Research Corp., Aliso Viejo, CA, USA). Data was processed using CrysAlisPro system software.[S3] The structure was solved by dual-space algorithm using SHELXT program[S4] through the Olex2 interface.[S5] All non-hydrogen atoms were refined anisotropically using a least-squares method, and hydrogen atoms were fixed at calculated positions and refined using a riding model. SHELXL−2014/7 was used for structure refinement.[S6] Full-matrix least-squares refinements on F^2 based on unique reflections with unweighted and weighted agreement factors of $R = \Sigma||F_o| - |F_c||/\Sigma|F_o|$ ($I > 2.00\ \sigma(I)$) and $wR = [\Sigma w(F_o^2 - F_c^2)^2/\Sigma w(F_o^2)^2]^{1/2}$ were performed. Mercury 4.0.0 was used for visualization and analysis of the structure. Crystallographic

data have been deposited with Cambridge Crystallographic Data Centre: Deposition numbers CCDC 2110898 for **CuTPFP**. Copies of the data can be obtained free of charge via www.ccdc.cam.ac.uk/data_request/cif.

2. Single crystal X-ray structure determination

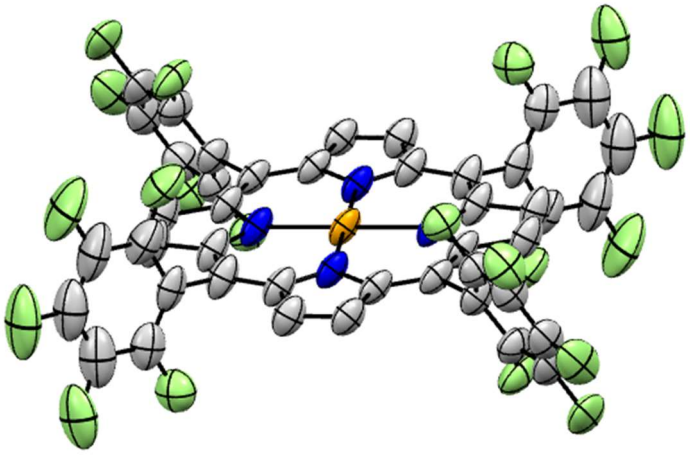

Fig. S1 ORTEP drawing of the structure of **CuTPFP**. Non-coordinated solvent molecules and hydrogen atoms have been omitted for clarity. Thermal ellipsoids are shown at the 50% level. C = grey, N = blue, F = light green and Cu = orange.

Table S1 Summary of crystallographic data for **CuTPFP**.

	CuTPFP
Formula	$C_{44}H_8CuF_{20}N_4 \cdot 2.0\ C_2H_3N$
Fw	1182.0
Crystal color, habit	Red, plate
Crystal size / nm^3	0.105 × 0.308 × 1.043
Crystal system	Monoclinic
Space group	$P\ 2_1/n$
a / Å	13.9205(7)
b / Å	11.2461(5)
c / Å	15.0429(6)
a / °	90
b / °	115.758(5)
g / °	90
V / $Å^3$	2120.99(18)
Z	2
F(000)	1106.0
d_{calc} / g cm^{-3}	1.751
μ(MoKa) / mm^{-1}	0.605
T / K	123(2)
R_1	0.0954
wR_2	0.2428
GooF	1.160

3. Electrochemical properties

The diffusion constant of **CuTPFP** at second peak is evaluated by the slope of Fig. S3b and Randles-Sevcik equation

$$I_{\mathrm{P}} = 0.4463nFAC^{*}_{\mathrm{cat}}\sqrt{\frac{nFv}{RT}}\sqrt{D_{\mathrm{cat}}}, \quad (1)$$

where n is the number of electrons (n = 1), F is the Faradaic constant (96485 C mol^{-1}), A is the electrode surface area (0.071 cm^2), C_{cat}^{*} is the concentration of the catalyst (mol cm^{-3}), R is the gas constant (8.31 J K^{-1} mol^{-1}), v is the scan rate (V s^{-1}), D_{cat} is the diffusion coefficient of the catalyst (cm^2 s^{-1}) and T is the temperature (298.15 K). As a result, D_{cat} = 7.58 × 10^{-6} cm^2 s^{-1}.

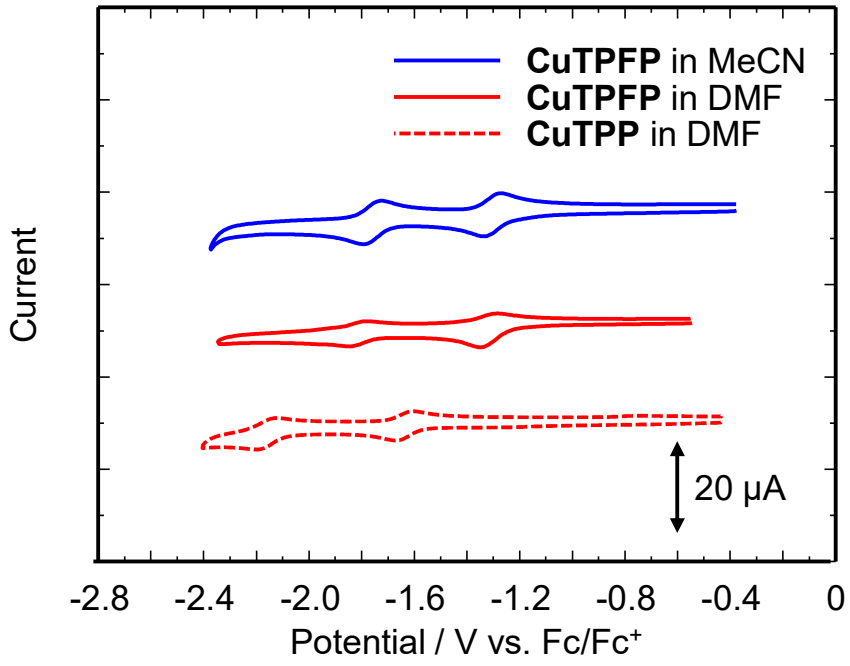

Fig. S2 Cyclic voltammograms of **CuTPFP** (0.2 mM) in MeCN (blue line) and DMF (red line) and of **CuTPP** in DMF (dashed line) with TBAP (0.1 M) under Ar (scan rate: 100 mV s^{-1}).

Table S2 Redox potentials ($E_{1/2}$/V vs. Fc/Fc$^+$) of **CuTPFP** in 0.1 M TBAP/MeCN, **CuTPFP** in 0.1 M TBAP/DMF and **CuTPP** in 0.1 M TBAP/DMF.

Catalyst	Solvent	$E_{1/2}$(1)	$E_{1/2}$(2)
CuTPFP	MeCN	–1.32	–1.77
CuTPFP	DMF	–1.32	–1.82
CuTPP	DMF	–1.64	–2.16

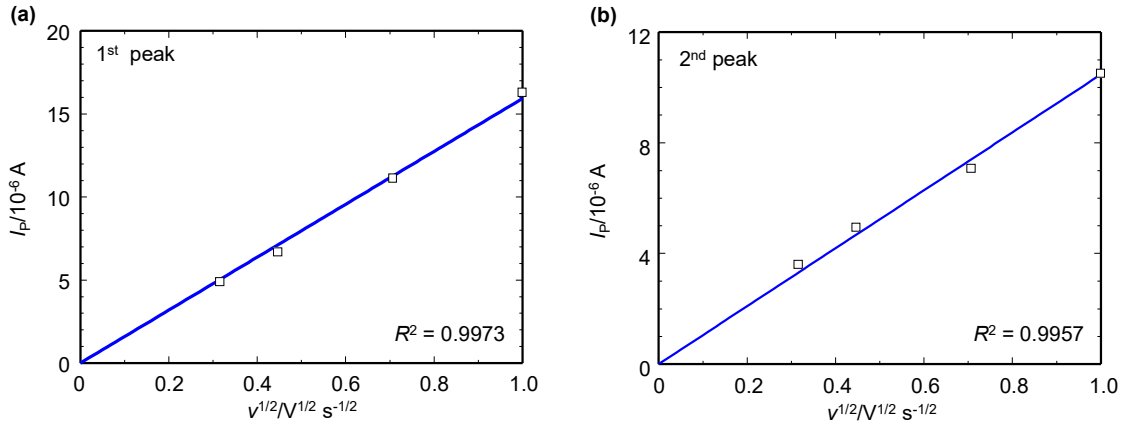

Fig. S3 Variation of peak current of **CuTPFP** (0.2 mM) in 0.1 M TBAP/MeCN (a) at the first redox wave (b) at the second redox wave.

4. Quantum chemical calculation

Quantum chemical calculation of the copper porphyrin complexes were performed to investigate the difference in reactivity between **CuTPFP** and **CuTPP**. B3LYP-D3[S7-S9] were used as a functional. Here, LANL2DZ (with core potential) basis set was used on copper, and 6-31G(*d*) basis set was used on the rest of the atoms (C, H, N and F). Solvation effects were included implicitly by the Continuum Polarized Conductor Model (CPCM), with a dielectric constant mimicking MeCN.[S10] All calculations were performed with the Gaussian 16 program package.[S11] Quantum chemical calculation revealed that the electronic structures of **CuTPFP** and **CuTPP** are largely different. The lowest unoccupied molecular orbital (LUMO) of **CuTPFP** was –3.03 eV, which is 0.28 eV lower than that of **CuTPP** (–2.75 eV). The LUMO of one electron reduced species of **CuTPFP** was also evaluated and the result was –2.18 eV, which is 0.35 eV lower than that of **CuTPP** (–1.83 eV). These results indicate that **CuTPFP** can receive electrons easier than **CuTPP**, which realizes low overpotential for electrochemical CO_2 reduction. Note that these tendencies are quite similar to that observed in the reduction potential in cyclic voltammograms (**CuTPFP**: –1.32 V and –1.77 V, **CuTPP**: –1.64 V and –2.16 V), indicating the validity of the calculation.

5. Controlled potential electrolysis experiment

CPE experiments were carried in a two-compartment cell separated by Nafion® membrane. The schematic representation of the experimental setup is shown in Fig. S4.

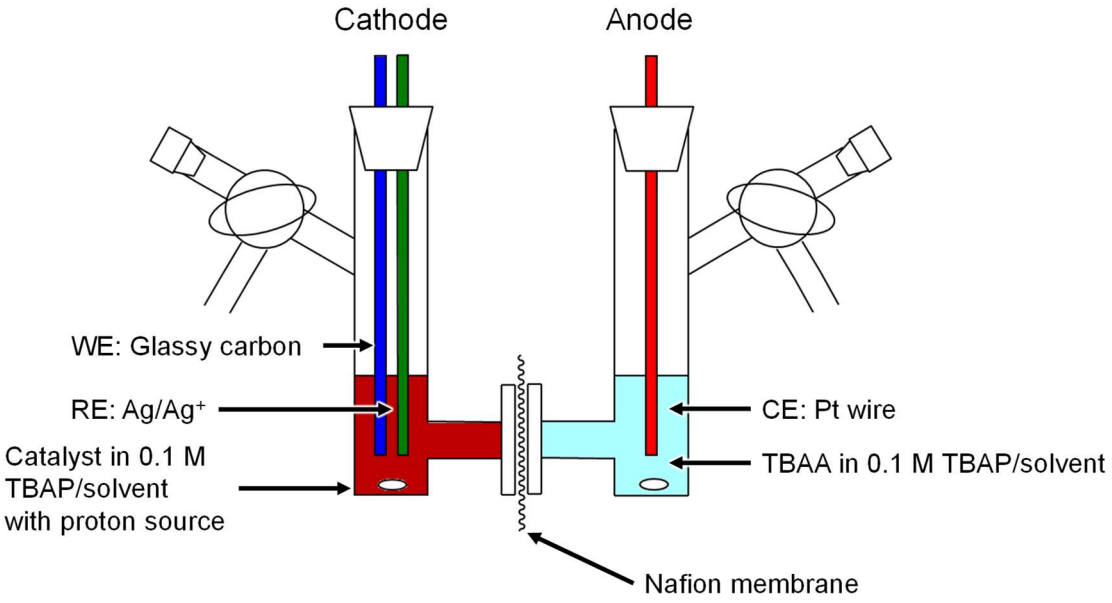

Fig. S4 Schematic representation of the custom-designed two compartment cell used in the controlled potential electrolysis experiments.

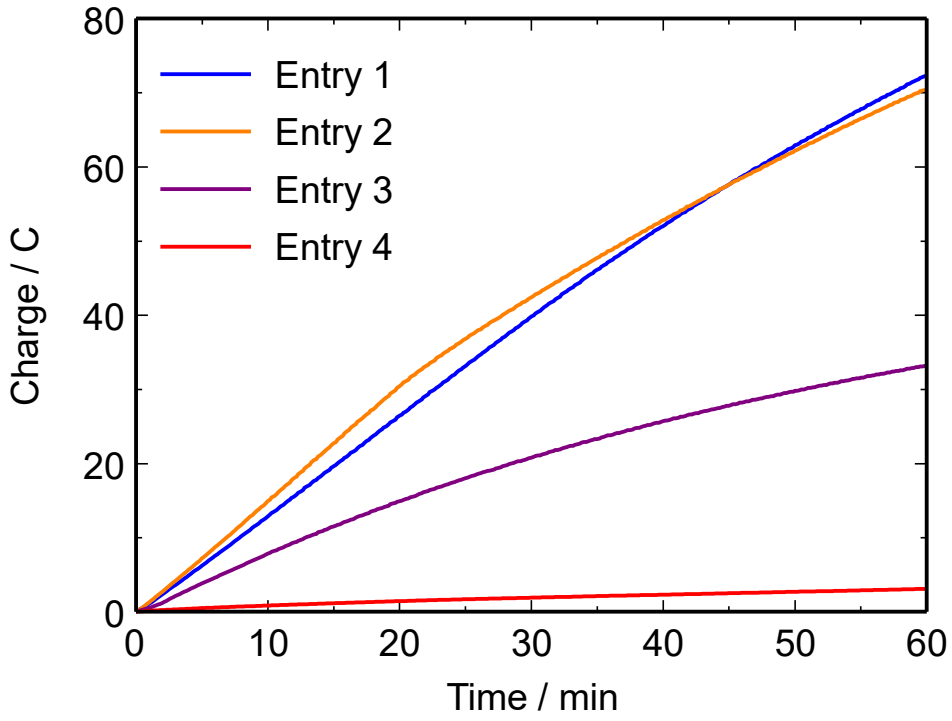

Fig. S5 The results of CPE experiments of **CuTPFP** (0.02 mM) at various applied potential (vs. Fc/Fc^+) for 1 h. Details of the experimental condition are summarized in Table S3. Working electrode: glassy carbon (1.2 cm^2), counter electrode: Pt wire, reference electrode: Ag/Ag^+.

Table S3 Summary of the CPE experiments of **CuTPFP** (0.02 mM).

Entry	Media	Potential / V vs. Fc/Fc^+	Total charge / C	Faradaic efficiency / %			
				CO	HCOOH	H_2	Total
1	0.1 M TBAP/MeCN, 1.0 M TFE	−2.39	72.4	76.6	19.6	1.7	98.2
2	0.1 M TBAP/MeCN, 1.0 M TFE	−2.20	70.5	75.9	16.6	4.1	95.8
3	0.1 M TBAP/MeCN, 1.0 M TFE	−2.03	33.2	56.3	22.1	7.6	90.2
4	0.1 M TBAP/MeCN, 1.0 M TFE	−1.71	3.1	18.7	4.3	13.5	63.0

6. Evidence for a homogeneous electrocatalyst

We confirmed the structure of molecular catalyst after the catalysis by the following several analyses.

6.1 Dynamic light scattering measurement after the CPE experiment

First, we performed a dynamic light scattering measurement of the solution after the CPE experiment (Fig. S6) and confirmed that there was no particle formation in the solution, which is evidence of the homogeneous nature of **CuTPFP**.

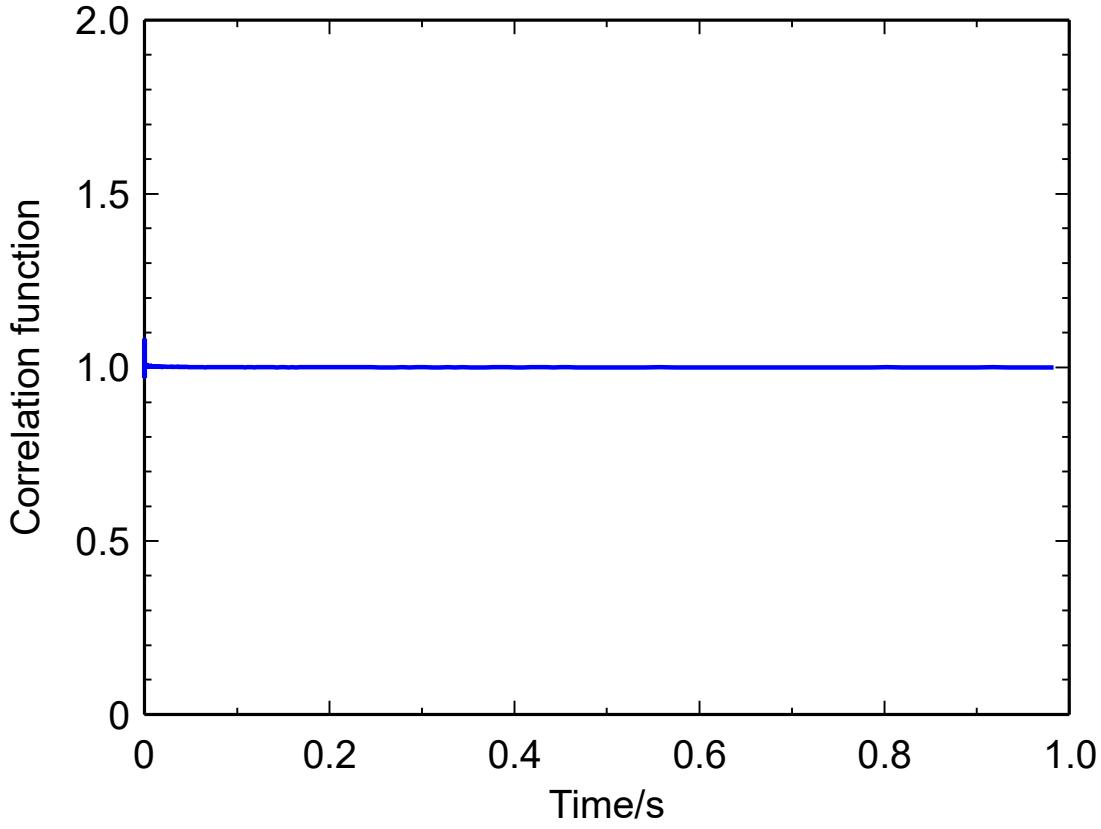

Fig. S6 Dynamic light scattering measurement of **CuTPFP** after the CPE experiment (Entry 1).

6.2 UV-visible absorption spectra before and after CPE experiments

Second, the UV-visible absorption spectra of **CuTPFP** were measured in acetonitrile (MeCN) with 0.1 M tetra-*n*-butylammonium perchlorate (TBAP) in the presence of 1.0 M TFE under CO_2 before and after controlled potential electrolysis (CPE) experiment at –2.40 V vs. Fc/Fc^+. As shown in Fig. S7, the electronic structure of **CuTPFP** was maintained after the electrolysis for 1h.

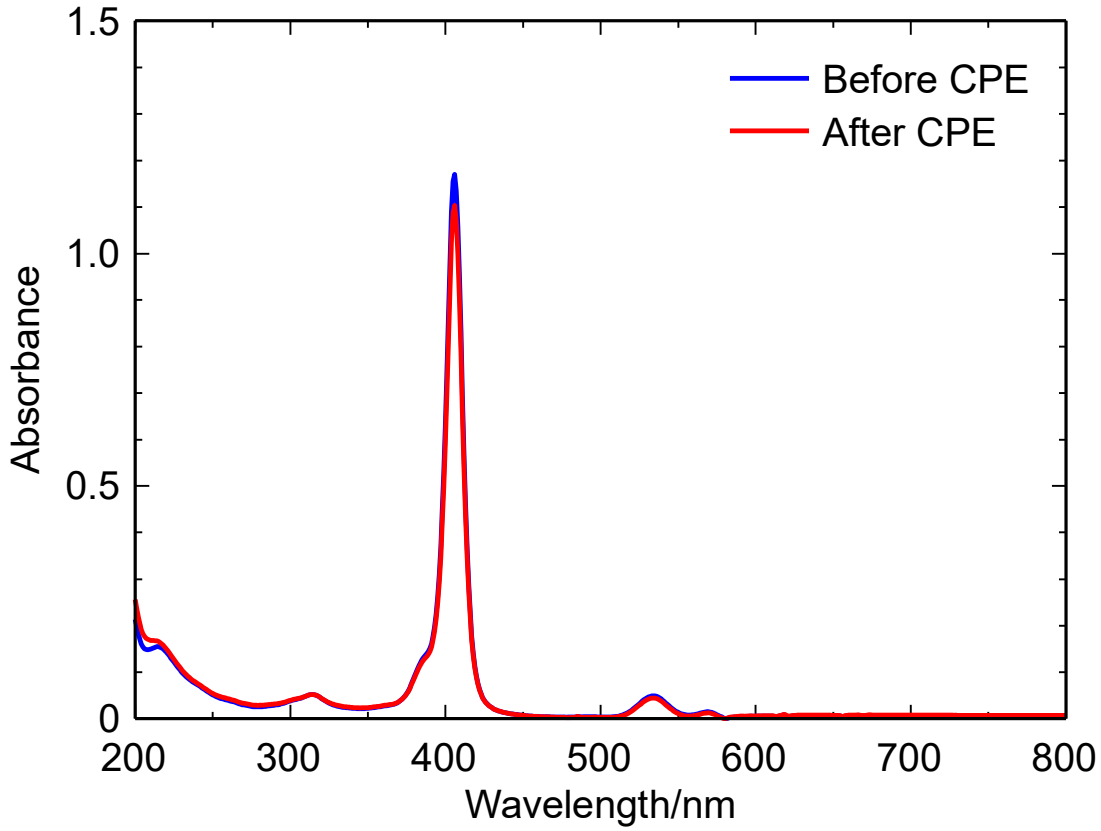

Fig. S7 UV-visible absorption spectra of **CuTPFP** in MeCN with 0.1 M TBAP in the presence of 1.0 M TFE under CO_2 before (blue line) and after (red line) the controlled potential electrolysis at –2.40 V vs. Fc/Fc^+ for 1h.

6.3 Catalytic ability of the electrode after the CPE experiment

Finally, we examined the catalytic ability of the electrode after the CPE experiment. The glassy carbon working electrode used in the electrolysis with catalyst (Fig. S8, blue line) was gently rinsed with small amount of MeCN, and then, a second round of electrolysis was performed using the solution without the catalyst (Fig. S8, black line). A small current was observed in the second electrolysis compared to the first electrolysis, and CO_2 reduction products were not observed (Table S4), which indicate that the homogeneous species dissolved in the solution is a catalytic active species.

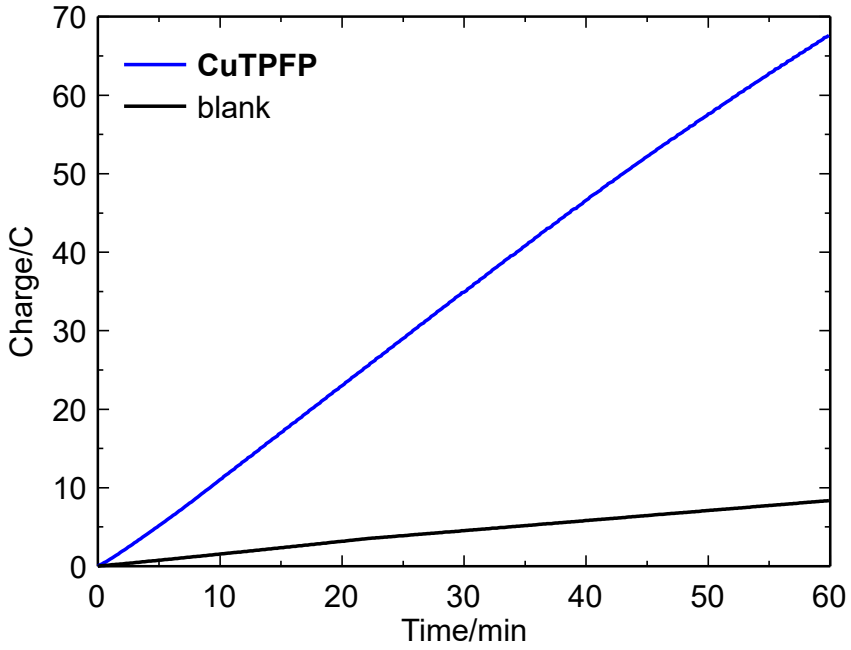

Fig. S8 The result of the first electrolysis using fresh glassy carbon electrode in 0.2 mM of **CuTPFP** (blue line) and that of second round of electrolysis using grassy carbon electrode after first electrolysis in electrolyte solution without **CuTPFP** (black line). Condition: MeCN solution with TBAP (0.1 M) under CO_2 in the presence of 1.0 M TFE at a potential of –2.40 V vs. Fc/Fc^+.

Table S4 Summary of the CPE experiments in Fig. S7.

Media	Catalyst/mM	Potential/ V vs. Fc/Fc^+	Total charge/C	Faradaic efficiency / %			
				CO	HCOOH	H_2	Total
0.1 M TBAP/MeCN, 1.0 M TFE	0.2	–2.40	67.7	72.6	24.7	2.6	99.9
0.1 M TBAP/MeCN, 1.0 M TFE	blank	–2.40	8.3	n.d.	trace	0.7	0.7

7. TOF calculation

The TOF values of the catalyst were evaluated based on following Eq.(2) and Eq.(3).[S12,S13] This is because in electrochemical condition, only small quantity of the catalyst close to the surface of the working electrode is catalytically active. These types of equations are often used for the evaluation of TOF values for molecule-based catalysts for CO_2 reduction, which reflects the inherent activity of the catalysts. In the following, definition of the equations for TOF calculation are described.

7.1 TOF calculation by CPE experiments

TOF value of the electrochemical CO_2 reduction is defined by

$$\mathrm{TOF} = \frac{k_{\mathrm{cat}}}{1 + \exp[f(E - E^0_{\mathrm{cat}})]}, \tag{2}$$

where k_{cat} is the observed rate constant, $f = F/RT$, E is the applied potential, and E^0_{cat} is the redox potential of the catalyst. Here, k_{cat} values were determined by CPE experiments using

$$I_{\mathrm{cat}} = \frac{nFAC^*_{\mathrm{cat}}\sqrt{k_{\mathrm{cat}}D_{\mathrm{cat}}}}{1 + \exp[f(E - E^0_{\mathrm{cat}})]}, \tag{3}$$

where I_{cat} is the average catalytic current during electrolysis, n is the number of electrons (n = 2), A is the electrode area (1.2 cm^2), F is the Faradaic constant (96485 C mol^{-1}), C_{cat}^* is the concentration of the catalyst (mol cm^{-3}), and D_{cat} is the diffusion coefficient of the catalyst (cm^2 s^{-1}). E^0_{cat}, D_{cat}, and C_{cat}^* of **CuTPFP** are –1.77 V vs. Fc/Fc^+, 7.58 × 10^{-6} cm^2 s^{-1} and 2.00 × 10^{-8} mol cm^{-3}, respectively (see pp. S8-9).

7.2 Catalytic Tafel plot

We have plotted TOF against overpotential (η) by using Eq. (4).

$$\mathrm{TOF} = \frac{\mathrm{TOF}_{\max}}{1 + \exp\left[f\left(E_{\mathrm{CO_2/CO}} - E^0_{\mathrm{cat}}\right)\right] \exp(-f\eta)}, \tag{4}$$

where $\mathrm{TOF}_{max} = k_{cat}$, $\eta = E - E_{CO2/CO}$, $E_{CO2/CO} = -1.54$ V vs. Fc/Fc^+.[S14,S15] As a result, catalytic Tafel plot shown in Fig. 2 was obtained (see the main text). Details are summarized in Table S5.

Table S5 TOF values of **CuTPFP** for electrochemical CO_2 reduction. The kinetic data was determined from the average of 1 h variable potential CPE experiments with direct product detections.

Entry	Media	Potential / V vs. Fc/Fc^+	η / V	TOF / s^{-1}	log TOF / s^{-1}
1	0.1 M TBAP/MeCN, 1.0 M TFE	–2.39	0.85	1.46×10^6	6.16
2	0.1 M TBAP/MeCN, 1.0 M TFE	–2.20	0.66	1.36×10^6	6.13
3	0.1 M TBAP/MeCN, 1.0 M TFE	–2.03	0.49	1.66×10^5	5.22
4	0.1 M TBAP/MeCN, 1.0 M TFE	–1.71	0.17	1.77×10^3	3.25

7.3 Comparison of TOF values on CO_2 reduction catalyst

TOF values in this work and those of recent efficient molecular catalysts are summarized in Table S6. Their structures are also described in Fig. S9. Details on how to calculate TOF is discussed in section 6.1 and 6.2 in this Supporting Information.

Table S6 TOFs of the recent efficient molecular catalysts for electrochemical CO_2 reduction.

Catalyst	Solvent	TOF_{max} (CV) / s^{-1} [a]	TOF (CPE) / s^{-1} [b]	Ref.
CuTPFP	0.1 M TBAP/MeCN, 1.0 M TFE	-	1,460,000[c] (–2.39 V *vs*. Fc/Fc^+)	This work
Fe1	0.1 M TBAP/MeCN, 1.0 M TFE	650,000[d]	7,300,000 (–2.35 V *vs*. Fc/Fc^+)	S16
Fe1	0.1 M $TBAPF_6$/DMF, 3.0 M PhOH	31,600	-	S17
Fe2	0.1 M $TBAPF_6$/DMF, 0.5 M PhOH	5,500,000	-	S18
Fe3	0.1 M $TBAPF_6$/DMF, 0.1 M H_2O + 3.0 M PhOH	1,000,000	-	S19
Fe4	0.1 M $TBAPF_6$/DMF, 0.1 M H_2O + 3.0 M PhOH	15,800	-	S19
Fe5	0.1 M $TBAPF_6$/DMF, 3.0 M PhOH	10,000	240 (–1.10 V *vs*. NHE)	S20
Fe6	0.1 M $TBAPF_6$/DMF, 3.0 M PhOH	6,300	170 (–1.16 V *vs*. NHE)	S20
Fe7	0.1 M $TBAPF_6$/MeCN, 3.5 M PhOH	-	900,000 (–1.98 V *vs*. Fc/Fc^+)	S21
Co1	0.1 M $TBAPF_6$/MeCN, 3.0 M PhOH	33,000	533 (–1.25 V *vs*. SCE)	S22
Mn1	0.1 M $TBAPF_6$/MeCN, 0.3 M TFE	5,011	-	S23
Ni1	0.1 M $TBAPF_6$/MeCN, 25% H_2O	-	190 (–1.16 V *vs*. NHE)	S24

[a] calculated from CV data. [b] calculated from CPE data. [c] TON (TOF × time, 1h) = 5.26×10^9, TON (mol(CO)/mol(catalyst) , 1h) = 2.87×10^3. [d] TOF_{max} is calculated using the data where $I_{cat}/I_p < 1$.

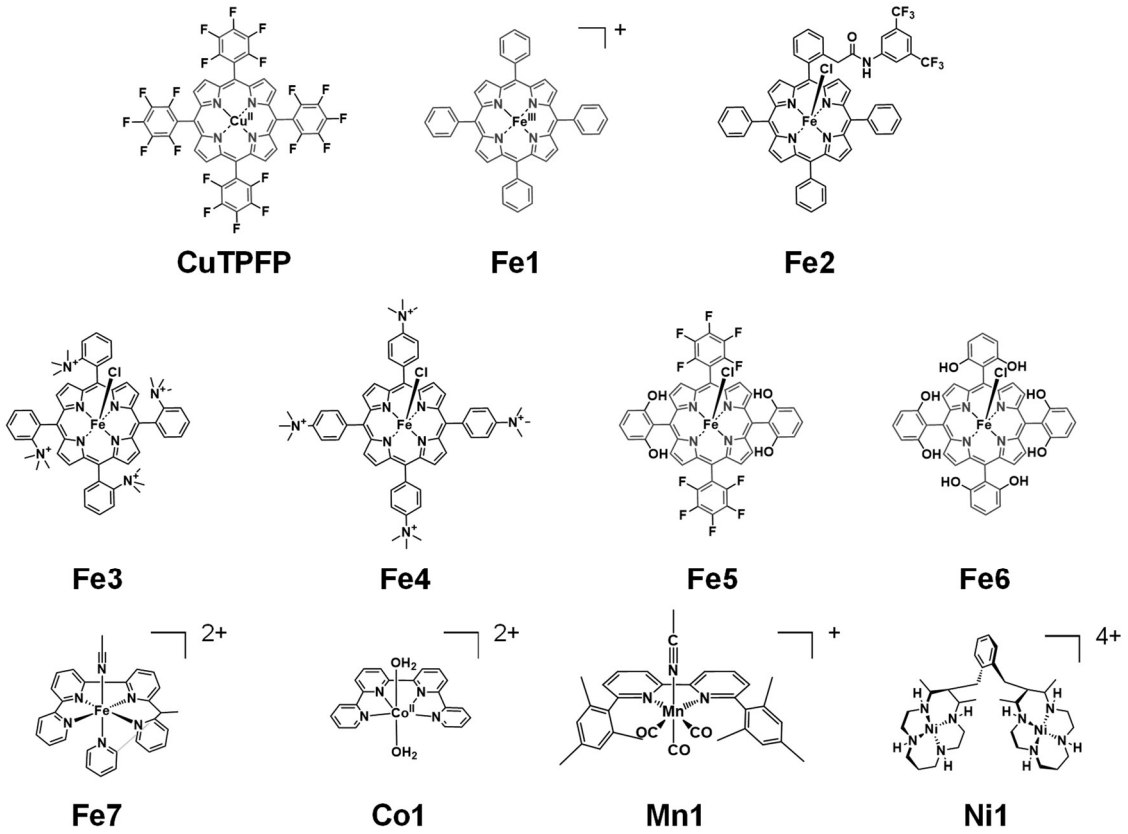

Fig. S9 Chemical structures of the catalysts in Table S6.

8. Catalytic ability of CuTPP

We have performed electrochemical measurements of **CuTPP** and evaluated TOF for CO production. As **CuTPP** did not dissolve in pure MeCN, the CPE was performed in MeCN-DMF [1:1 (v/v)] mixed solvent system.

8.1 Cyclic voltammetry measurement of CuTPP

First, we performed cyclic voltammetry measurement of **CuTPP**. Under Ar, **CuTPP** exhibited two redox potentials at –1.65 V and –2.13 V (Fig. S10a, red line). The peak currents corresponding to these redox potentials of **CuTPP** have a linear relationship with the square root of the scan rate and follow the Randles–Sevcik equation, indicating that **CuTPP** can facilitate rapid electron transfer reactions (Fig. S10b). Using Eq.(1) and the slope of Fig. S10b, D_{cat} of **CuTPP** is 9.24×10^{-6} cm^2 s^{-1}. Under CO_2 in the presence of TFE, **CuTPP** exhibited an irreversible current, suggesting the electrocatalytic activity of the complex for CO_2 reduction (Fig. S10a, blue line).

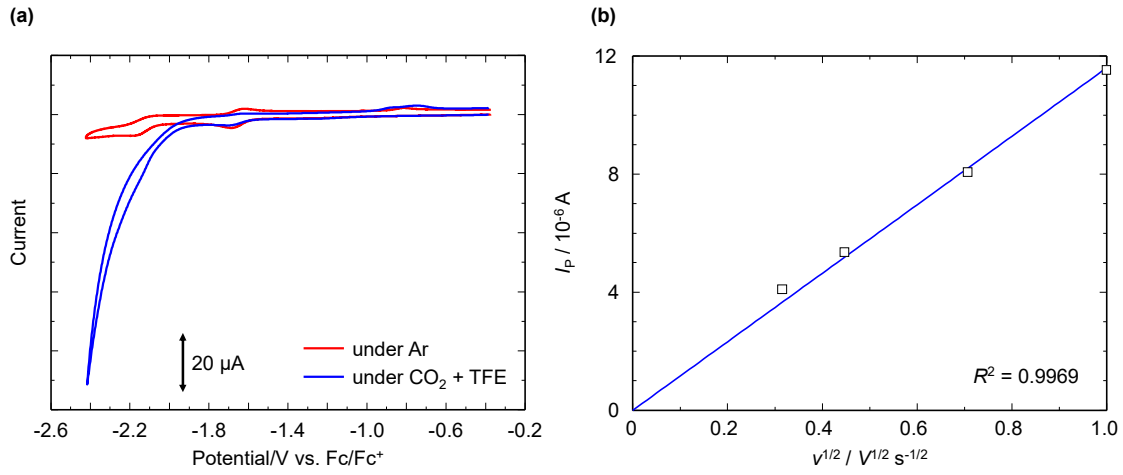

Fig. S10 (a) Cyclic voltammograms of **CuTPP** (0.2 mM) in DMF/MeCN [1:1 (v/v)] mixed solvent with TBAP (0.1 M) under Ar (red line) and under CO_2 in the presence of 0.5 M TFE (blue line). Scan rate: 100 mV s^{-1}. (b) Variation of peak current of **CuTPP** (0.2 mM) in DMF/MeCN [1:1 (v/v)] mixed solvent with TBAP (0.1 M) under Ar at the second redox wave.

8.2 CPE experiment of CuTPP

We performed CPE experiment of **CuTPP** at –2.39 V. As a result, the total amount of charge passed over a period of 60 min was 8.4 C (Fig. S11 and Table S7). The products of the reaction were quantified and the formation of CO, HCOOH, and H_2 was confirmed with a Faradaic efficiency of 81.5%, 17.1% and 1.0%, respectively.

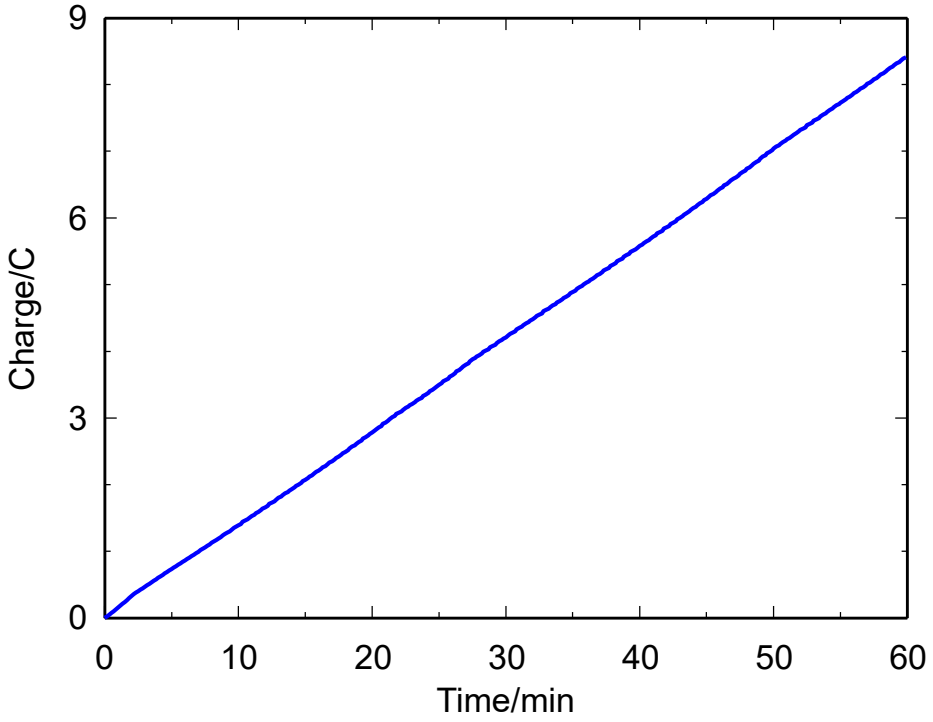

Fig. S11 The result of CPE experiment of **CuTPP** (0.02 mM) at –2.39 V for 1h. Working electrode, glassy carbon (1.2 cm^2); counter electrode, Pt wire; reference electrode, Ag/Ag+.

Table S7 Summary of the CPE experiment of **CuTPP**.

Media	Catalyst/m M	Potential/ V vs. Fc/Fc^+	Total charge/C	Faradaic efficiency / %			
				CO	HCOOH	H_2	Total
DMF/MeCN [1:1 (v/v)], 0.1 M TBAP, 1.0 M TFE	0.02	–2.39	8.4	81.5	17.1	1.0	99.6

8.3 TOF of CuTPP

Based on the result of CPE experiment and Eq.(2), we evaluated TOF of **CuTPP**. As a result, the TOF value of **CuTPP** for CO production at –2.39 V was 1.82×10^4 s^{-1}, which is much lower than that of **CuTPFP** (TOF = 1.46×10^6 s^{-1} at –2.39 V).

9. References

S1. A. D. Alder, F. R. Long, W. Shergalis, *J. Am. Chem. Soc.* **1964**, *86*, 3145.

S2. S. L. Rebelo, A. M. N. Silva, C. J. Medforth, C. Freire, *Molecules* **2016**, *21*, 481.

S3. CrysAlisPro, Oxford Diffraction Ltd., Version 1.171.39.46.

S4. G. M. Sheldrick, *Acta Cryst.* **2015**, A71, 3.

S5. O. V. Dolomanov, L. J. Bourhis, R. J. Gildea, J. A. K. Howard, H. Puschmann, *J. Appl. Crystallogr.* **2009**, *42*, 339.

S6. G. M. Sheldrick, *Acta Cryst.* 2015, A71, 3.

S7. A. D. Becke, *J. Chem. Phys.* **1993**, *98*, 5648.

S8. C. Lee, W. Yang, R. G. Parr, *Phys. Rev. B.* **1988**, *37*, 785.

S9. S. Grimme, *J. Chem. Phys.* **2006**, *124*, 034108.

S10. J. Tomasi, B. Mennucci, R. Cammi, *Chem. Rev.* **2005**, *105*, 2999.

S11. *Gaussian 16*, Revision C.01, M. J. Frisch, G. W. Trucks, H. B. Schlegel, G. E. Scuseria, M. A. Robb, J. R. Cheeseman, G. Scalmani, V. Barone, G. A. Petersson, H. Nakatsuji, X. Li, M. Caricato, A. V. Marenich, J. Bloino, B. G. Janesko, R. Gomperts, B. Mennucci, H. P. Hratchian, J. V. Ortiz, A. F. Izmaylov, J. L. Sonnenberg, D. Williams-Young, F. Ding, F. Lipparini, F. Egidi, J. Goings, B. Peng, A. Petrone, T. Henderson, D. Ranasinghe, V. G. Zakrzewski, J. Gao, N. Rega, G. Zheng, W. Liang, M. Hada, M. Ehara, K. Toyota, R. Fukuda, J. Hasegawa, M. Ishida, T. Nakajima, Y. Honda, O. Kitao, H. Nakai, T. Vreven, K. Throssell, J. A. Montgomery, Jr., J. E. Peralta, F. Ogliaro, M. J. Bearpark, J. J. Heyd, E. N. Brothers, K. N. Kudin, V. N. Staroverov, T. A. Keith, R. Kobayashi, J. Normand, K. Raghavachari, A. P. Rendell, J. C. Burant, S. S. Iyengar, J. Tomasi, M. Cossi, J. M. Millam, M. Klene, C. Adamo, R. Cammi, J. W. Ochterski, R. L. Martin, K. Morokuma, O. Farkas, J. B. Foresman, and D. J. Fox, Gaussian, Inc., Wallingford CT, 2016.

S12. C. Costentin, S. Drouet, M. Robert, J. M. Savéant, *J. Am. Chem. Soc.* **2012**, *134*, 11235.

S13. C. Costentin, J. M. Savéant, *ChemElectroChem.* **2014**, *1*, 1226.

S14. M. L. Pegis, J. A. S. Roberts, D. J. Wasylenko, E. A. Mader, A. M. Appel, J. M. Mayer, *Inorg. Chem.* **2015**, *54*, 11883.

S15. S. Sonha, J. J. Warren, *Inorg. Chem.* **2018**, *57*, 12650.

S16. K. Kosugi, M. Kondo, S. Masaoka, *Angew. Chem. Int. Ed.* **2021**, *in press*. (DOI: 10.1002/anie.202110190).

S17. C. Costentin, S. Drouet, G. Passard, M. Robert, J. M. Savéant, *J. Am. Chem. Soc.* **2013**, *135*, 9023.

S18. E. M. Nichols, J. S. Derrick, S. K. Nistanaki, P. T. Smith, C. J. Chang, *Chem. Sci.* **2018**, *9*, 2952.

S19. I. Azcarate, C. Costentin, M. Robert, J. M. Savéant, *J. Am. Chem. Soc.* **2016**, *138*, 16639.

S20. C. Costentin, G. Passard, M. Robert, J. M. Savéant, *Proc. Natl. Acad. Sci. USA*, **2014,** *111*, 14990.

S21. J. S. Derrick, M. Loipersberger, R. Chatterjee, D. A. Iovan, P. T. Smith, K. Chalarawet, J. Yano, J. R. Long, M. Head-Gordon, C. J. Chang, *J. Am. Chem. Soc.* **2020**, *142*, 20489.

S22. C. Cometto, L. Chen, P. K. Lo, Z. Guo, K. C. Lau, E. Anxolabéhère-Mallart, C. Fave, T. C. Lau, M. Robert, *ACS Catal*. **2018**, *8*, 3411.

S23. M. D. Sampson, C. P. Kubiak, *J*. *Am*. *Chem*. *Soc*. **2016**, *138*, 1386.

S24. L. M. Cao, H. H. Huang, J. W. Wang, D. C. Zhong, T. B. Lu, *Green*. *Chem*. **2018**, *20*, 798.